Modeling blue and green water availability in Africa

Jürgen Schuol,[1,2] Karim C. Abbaspour,[1] Hong Yang,[1] Raghavan Srinivasan,[3] and Alexander J. B. Zehnder[4]

[1] Despite the general awareness that in Africa many people and large areas are suffering from insufficient water supply, spatially and temporally detailed information on freshwater availability and water scarcity is so far rather limited. By applying a semidistributed hydrological model SWAT (Soil and Water Assessment Tool), the freshwater components blue water flow (i.e., water yield plus deep aquifer recharge), green water flow (i.e., actual evapotranspiration), and green water storage (i.e., soil water) were estimated at a subbasin level with monthly resolution for the whole of Africa. Using the program SUFI-2 (Sequential Uncertainty Fitting Algorithm), the model was calibrated and validated at 207 discharge stations, and prediction uncertainties were quantified. The presented model and its results could be used in various advanced studies on climate change, water and food security, and virtual water trade, among others. The model results are generally good albeit with large prediction uncertainties in some cases. These uncertainties, however, disclose the actual knowledge about the modeled processes. The effect of considering these model-based uncertainties in advanced studies is shown for the computation of water scarcity indicators.

Citation: Schuol, J., K. C. Abbaspour, H. Yang, R. Srinivasan, and A. J. B. Zehnder (2008), Modeling blue and green water availability in Africa, *Water Resour. Res.*, *44*, W07406, doi:10.1029/2007WR006609.

1. Introduction

[2] On a continental and annual basis Africa has abundant water resources but the problem is their high spatial and temporal variability within and between countries and river basins [*UN-Water/Africa*, 2006]. Considering this variability, the continent can be seen as dry with pressing water problems [*Falkenmark*, 1989; *Vörösmarty et al.*, 2005]. Though of critical importance, detailed information on water resources and water scarcity is still limited in Africa [*Wallace and Gregory*, 2002].

[3] Freshwater availability is a prerequisite for food security, public health, ecosystem protection, etc. Thus freshwater is important and relevant for achieving all development goals contained in the United Nations Millennium Declaration (http://www.un.org/millennium/declaration/ares552e.pdf). Two important targets of the Declaration are to halve, by the year 2015, the proportion of people without sustainable access to safe drinking water and to halve the proportion of people who suffer from hunger. These two targets are closely related to freshwater availability.

[4] Up to now, studies of freshwater availability have predominantly focused on the quantification of the "blue water", while ignoring the "green water" as part of the water resource and its great importance especially for rainfed agriculture (e.g., in sub-Saharan Africa more than 95% is rainfed [*Rockström et al.*, 2007]). Two of the few studies dealing with green water are *Rockström and Gordon* [2001] and *Gerten et al.* [2005]. Blue water flow, or the internal renewable water resource (IRWR), is traditionally quantified as the sum of the water yield and the deep aquifer recharge. Green water, on the other hand, originates from the naturally infiltrated water, which is more and more being thought of as a manageable water resource. *Falkenmark and Rockström* [2006] differentiate between two components of the green water: green water resource (or storage), which equals the moisture in the soil, and green water flow, which equals the sum of the actual evaporation (the nonproductive part) and the actual transpiration (the productive part). In some references only the transpiration is regarded as the green water component [e.g., *Savenije*, 2004]. As evaporation and transpiration are closely interlinked processes and evaporated water has the potential to be partly used as productive flow for food production, we prefer to consider the total actual evapotranspiration as the green water flow.

[5] Spatially and temporally detailed assessments of the different components of freshwater availability are essential for locating critical regions, and thus, the basis for rational decision-making in water resources planning and management. There exist already a few global freshwater assessments based on (1) data generalization [e.g., *Shiklomanov*, 2000; *Shiklomanov and Rodda*, 2003], (2) general circulation models (GCMs), [e.g., TRIP, *Oki et al.*, 2001; *Oki and*

[1]Department System Analysis, Integrated Assessment and Modelling, Eawag, Swiss Federal Institute of Aquatic Science and Technology, Dübendorf, Switzerland.

[2]Swiss Federal Institute of Technology, Zürich, Switzerland.

[3]Spatial Sciences Laboratory, Texas A&M University, Texas Agricultural Experimental Station, College Station, Texas, USA.

[4]Board of the Swiss Federal Institutes of Technology, ETH-Zentrum, Zürich, Switzerland.

Kanae, 2006], and (3) hydrological models [e.g., WBM, *Vörösmarty et al.*, 1998, 2000; *Fekete et al.*, 1999; Macro-PDM, *Arnell*, 1999; WGHM (WaterGAP 2), *Alcamo et al.*, 2003; *Döll et al.*, 2003; LPJ, *Gerten et al.*, 2004; WAS-MOD-M, *Widén-Nilsson et al.*, 2007]. GCMs with their strength on the atmospheric model component perform poorly on the soil water processes [*Döll et al.*, 2003]. All the above mentioned hydrological models are raster models with a spatial resolution of 0.5° but show different degrees of complexities. These models either have not been calibrated (e.g., WBM) or only one (e.g., WGHM) or few parameters (e.g., WASMOD-M) have been checked and adjusted against long-term average runoffs. In WGHM, for some basins one or two correction factors have been additionally applied in order to guarantee a maximum of 1% error of the simulated long-term annual average runoff [*Döll et al.*, 2003]. Intraannual runoff differences, which are of key importance in many regions have been included in some studies [e.g., *Widén-Nilsson et al.*, 2007] but not used for calibration.

[6] The existing global and continental freshwater assessment models have been used for climate and socio-economic change scenarios [*Alcamo et al.*, 2007], water stress computation [*Vörösmarty et al.*, 2005], analysis of seasonal and interannual continental water storage variations [*Güntner et al.*, 2007], global water scarcity analysis taking into account environmental water requirements [*Smakhtin et al.*, 2004], and virtual water trading [*Islam et al.*, 2007] among others. Hence it is important that these models pass through a careful calibration, validation, and uncertainty analysis. Particularly in large-scale (hydrological) models, the expected uncertainties are rather large. For this task, several different procedures have been developed: e.g., Generalized Likelihood Uncertainty Estimation (GLUE) [*Beven and Binley*, 1992], Bayesian inference based on Markov Chain Monte Carlo (MCMC) [*Vrugt et al.*, 2003], Parameter Solution (ParaSol) [*van Griensven and Meixner*, 2006], and Sequential Uncertainty Fitting (SUFI-2) [*Abbaspour et al.*, 2007].

[7] In this study, we modeled the monthly subcountry-based freshwater availability for Africa and explicitly differentiated between the different freshwater components: blue water flow, green water storage and green water flow. The model of choice was "Soil and Water Assessment Tool" (SWAT) [*Arnold et al.*, 1998] because of two reasons. First, SWAT has been already successfully applied for water quantity and quality issues for a wide range of scales and environmental conditions around the globe. A comprehensive SWAT review paper summarizing the findings of more than 250 peer-reviewed articles is written by *Gassman et al.* [2007]. The suitability of SWAT for very large scales applications has been shown in the "Hydrologic Unit Model for the United States" project (HUMUS) [*Arnold et al.*, 1999; *Srinivasan et al.*, 1998]. SWAT was recently also applied in the national and watershed assessments of the U.S. Department of Agriculture (USDA) Conservation Effects Assessment Program (CEAP, http://www.nrcs.usda.gov/Technical/nri/ceap/index.html). The second reason for choosing SWAT for this exclusive water quantity study was its ability to perform plant growth and water quality modeling, a topic we plan to study in the future. An advantage of SWAT is its modular implementation where

processes can be selected or not. As processes are represented by parameters in the model, in data scarce regions SWAT can run with a minimum number of parameters. As more is known about a region, more processes can be invoked for by updating and running the model again.

[8] The African model was calibrated and validated at 207 discharge stations across the continent. Uncertainties were quantified using SUFI-2 program [*Abbaspour et al.*, 2007]. *Yang et al.* [2008] compared different uncertainty analysis techniques in connection to SWAT and found that SUFI-2 needed the smallest number of model runs to achieve a similarly good solution and prediction uncertainty. This efficiency issue is of great importance when dealing with computationally intensive, complex, and large-scale models. In addition, SUFI-2 is linked to SWAT (in the SWAT-CUP software) [*Abbaspour et al.*, 2008] through an interface that includes also the programs GLUE, ParaSol, and MCMC.

2. Materials and Methods

2.1. SWAT2005 Model and ArcSWAT Interface

[9] To simulate the water resources availability in Africa, the latest version of the semiphysically based, semidistributed, basin-scale model SWAT [*Arnold et al.*, 1998] was selected (SWAT2005) [*Neitsch et al.*, 2005]. SWAT is a continuous time model and operates on a daily time step. Only the hydrologic component of the model was used in this study. In SWAT the modeled area is divided into multiple subbasins by overlaying elevation, land cover, soil, and slope classes. In this study the subbasins were characterized by dominant land-use, soil, and slope classes. This choice was essential for keeping the size of the model at a practical limit. For each of the subunits, water balance was simulated for four storage volumes: snow, soil profile, shallow aquifer, and deep aquifer. In our case, potential evapotranspiration was computed using the Hargreaves method which requires the climatic input of daily precipitation, and minimum and maximum temperature. Surface runoff was simulated using a modification of the SCS Curve Number (CN) method. Despite the empirical nature, this approach has been proven to be successful for many applications and a wide variety of hydrologic conditions [*Gassman et al.*, 2007]. The runoff from each subbasin was routed through the river network to the main basin outlet using, in our case, the variable storage method. Further technical model details are given by *Arnold et al.* [1998] and *Neitsch et al.* [2005].

[10] The preprocessing of the SWAT model input (e.g., watershed delineation, manipulation of the spatial and tabular data) was performed within ESRI ArcGIS 9.1 using the ArcSWAT interface [*Winchell et al.*, 2007]. In comparison to the ArcView GIS interface AVSWAT2000 [*Di Luzio et al.*, 2001], ArcSWAT has no apparent limitation concerning the size and complexity of the simulated area as it was able to model the entire African continent.

2.2. Calibration and Uncertainty Analysis Procedure SUFI-2

[11] The program SUFI-2 [*Abbaspour et al.*, 2007] was used for a combined calibration and uncertainty analysis. In any (hydrological) modeling work there are uncertainties in input (e.g., rainfall), in conceptual model (e.g., by process

simplification or by ignoring important processes), in model parameters (nonuniqueness) and in the measured data (e.g., discharge used for calibration). SUFI-2 maps the aggregated uncertainties to the parameters and aims to obtain the smallest parameter uncertainty (ranges). The parameter uncertainty leads to uncertainty in the output which is quantified by the 95% prediction uncertainty (95PPU) calculated at the 2.5% (L95PPU) and the 97.5% (U95PPU) levels of the cumulative distribution obtained through Latin hypercube sampling. Starting with large but physically meaningful parameter ranges that bracket 'most' of the measured data within the 95PPU, SUFI-2 decreases the parameter uncertainties iteratively. After each iteration, new and narrower parameter uncertainties are calculated [see *Abbaspour et al.*, 2007] where the more sensitive parameters find a larger uncertainty reduction than the less sensitive parameters. In deterministic simulations, output (i.e., river discharge) is a signal and can be compared to a measured signal using indices such as R^2, root mean square error, or Nash-Sutcliffe. In stochastic simulations where predicted output is given by a prediction uncertainty band instead of a signal, we devised two different indices to compare measurement to simulation: the *P-factor* and the *R-factor* [*Abbaspour et al.*, 2007]. These indices were used to gauge the strength of calibration and uncertainty measures. The *P-factor* is the percentage of measured data bracketed by the 95PPU. As all correct processes and model inputs are reflected in the observations, the degree to which they are bracketed in the 95PPU indicates the degree to which the model uncertainties are being accounted for. The maximum value for the *P-factor* is 100%, and ideally we would like to bracket all measured data, except the outliers, in the 95PPU band. The *R-factor* is calculated as the ratio between the average thickness of the 95PPU band and the standard deviation of the measured data. It represents the width of the uncertainty interval and should be as small as possible. *R-factor* indicates the strength of the calibration and should be close to or smaller than a practical value of 1. As a larger *P-factor* can be found at the expense of a larger *R-factor*, often a trade off between the two must be sought.

2.3. Database

[12] The model for the continent of Africa was constructed using in most cases freely available global information. The collection of the data was followed by an accurate compilation and analysis of the quality and integrity. The basic input maps included the digital elevation model (DEM) GTOPO30, the digital stream network HYDRO1k (http://edc.usgs.gov/products/elevation/gtopo30/hydro/index.html), and the land cover map Global Land Cover Characterization (GLCC) (http://edcsns17.cr.usgs.gov/glcc/) both at a resolution of 1 km from U.S. Geological Survey (USGS). The soil map was produced by the Food and Agriculture Organization of the United Nations [*FAO*, 1995] at a resolution of 10 km, including almost 5000 soil types and two soil layers. Because of the few and unevenly distributed weather stations in Africa with often only short and erroneous time series, the daily weather input (precipitation, minimum and maximum temperature) was generated for each subbasin based on the 0.5° grids monthly statistics from Climatic Research Unit (CRU TS 1.0 and 2.0, http://www.cru.uea.ac.uk/cru/data/hrg.htm). We developed a semi-automated weather generator, dGen, for this purpose [*Schuol and Abbaspour*, 2007]. Information on lakes, wetlands and reservoirs was extracted from the Global Lakes and Wetlands Database (GLWD) [*Lehner and Döll*, 2004]. River discharge data, which is essential for calibration and validation, were obtained from the Global Runoff Data Centre (GRDC, http://grdc.bafg.de). More details on the databases are discussed by *Schuol et al.* [2008].

2.4. Model Setup

[13] The ArcSWAT interface was used for the setup and parameterization of the model. On the basis of the DEM and the stream network, a minimum drainage area of 10,000 km^2 was chosen to discretize the continent into 1496 subbasins. The geomorphology, stream parameterization, and overlay of soil and land cover were automatically done within the interface. To mitigate the effect of land cover change over time, and to decrease the computational time of the very large-scale model, the dominant soil and land cover were used in each subbasin. The simulation period was from 1968 to 1995 and for these years we provided daily generated weather input. The first 3 years were used as warm-up period to mitigate the unknown initial conditions and were excluded from the analysis. Lakes, wetlands, and reservoirs, which affect the river discharge to a great extent, were also included in the model. As detail information was lacking, only 64 reservoirs with storage volumes larger than 1 km^3 were included (Figure 1). In this study, wetlands on the main channel networks as well as lakes were treated as reservoirs. The parameterization was mostly based on information from GLWD-1 [*Lehner and Döll*, 2004].

2.5. Model Calibration Procedures

[14] Model calibration and validation is a necessary, challenging but also to a certain degree subjective step in the development of any complex hydrological model. The African model was calibrated using monthly river discharges from 207 stations. These stations were unevenly distributed throughout the continent (Figure 1) and covered, in most cases, only parts of the whole analysis period from 1971 to 1995. For this reason it was inevitable to include different time lengths (minimum of 3 years) and time periods at the different stations in the calibration procedure. Consistently at all stations, using a split-sample procedure, the more recent half of the discharge data were used for calibration and the prior half were used for validation. In order to compare the monthly measured and simulated discharges, Φ, a weighted version of the coefficient of determination (slightly modified [*Krause et al.*, 2005]) was selected as efficiency criteria:

$$\Phi = \begin{cases} |b|R^2 & \text{if } |b| \leq 1 \\ |b|^{-1}R^2 & \text{if } |b| > 1 \end{cases} \tag{1}$$

where the coefficient of determination R^2 represents the discharge dynamics, and b is the slope of the regression line between the monthly observed and simulated runoff. Including b guarantees that runoff under- or over-predictions are also reflected. A major advantage of this efficiency criterion is that it ranges from 0 to 1, which compared to Nash-Sutcliff coefficient with a range of $-\infty$ to 1, ensures
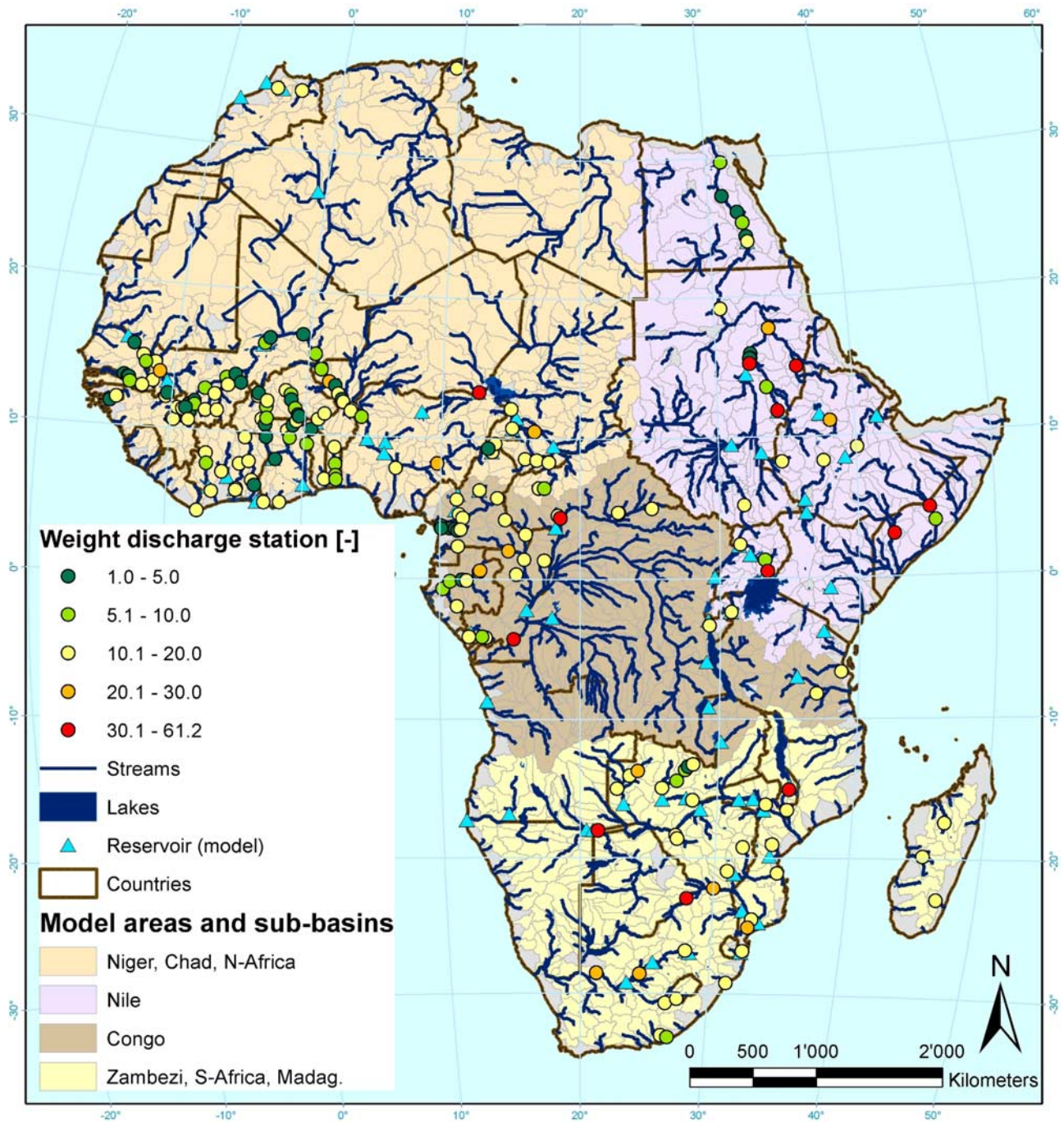
Figure 1. Location of the reservoirs included in the model and the four model areas used in the third calibration procedure. Also shown are the discharge stations and their associated weights in the calibration.

that in a multisite calibration the objective function is not governed by a single or a few badly simulated stations.

[15] In order to obtain some knowledge of the uncertainty associated with the selected calibration method, three independent calibrations were performed, each having a different objective function. In the first procedure the objective function was formulated as the n-station-sum of Φ:

$$g = \sum_{i=1}^{n} \Phi_i \qquad (2)$$

[16] In the second procedure, each station was weighted (w) depending on the contributing area A in km^2 and the number of monthly observations s used for calibration at a certain station i and the upstream stations j:

$$g = \sum_{i=1}^{n} (w_i \cdot \Phi_i) \qquad (3)$$

Table 1. Soil Texture and Land Cover Distribution Within the Modeled African Basin and the Four Subareas

	Abbreviation	Africa, %	Area 1, %	Area 2, %	Area 3, %	Area 4, %
Land cover						
Barren or sparsely vegetated	BSVG	32.7	58.6	35.6	...	0.6
Dryland cropland and pasture	CRDY	4.3	0.3	3.9	5.9	12.5
Cropland/grassland mosaic	CRGR	1.3	...	...	...	7.3
Cropland/woodland mosaic	CRWO	2.4	1.8	2.6	5.1	0.7
Deciduous broadleaf forest	FODB	3.2	...	...	11.8	6.2
Evergreen broadleaf forest	FOEB	8.6	0.9	...	46.7	0.6
Mixed forest	FOMI	0.1	...	...	0.9	...
Grassland	GRAS	5.9	6.7	2.1	0.0	14.0
Mixed grassland/shrubland	MIGS	0.6	1.3	...	...	...
Savannah	SAVA	30.0	26.9	30.2	27.1	39.5
Shrubland	SHRB	9.4	3.4	22.3	...	16.5
Water bodies	WATB	1.5	...	3.0	2.4	2.1
Herbaceous wetland	WEHB	0.0	...	0.2	...	...
Soil						
Clay	C	8.7	0.8	17.5	20.8	4.7
Clay-loam	CL	11.3	17.8	10.6	3.4	4.8
Loam	L	29.9	42.9	30.0	9.7	19.0
Loamy-sand	LS	5.0	4.3	0.0	14.4	3.4
Sand	S	2.6	3.7	4.7	...	0.0
Sandy-clay-loam	SCL	19.0	11.8	17.1	32.4	25.0
Sandy-loam	SL	23.5	18.6	19.7	19.2	43.2
Silt-loam	IL	0.1	...	0.4	...	...
Silty-clay	IC	0.0	0.0	...	...	...

where

$$w_i = \sqrt{\frac{\left(A_i - \sum_{j=1}^{n} A_j\right) \cdot s_i}{s_i + \sum_{j=1}^{n} s_j}} \qquad (4)$$

[17] The idea behind this weighting is that a runoff station with a long data series and a large watershed without further stations upstream provides more information for calibration and should have a larger weight than a station in a densely gauged area or a station with a short time series. The weights ranged from 1 to 61 for the furthest downstream station on the river Congo at Kinshasa (Figure 1).

[18] In the third calibration procedure the region was divided into four modeling zones and each zone was calibrated independently. The four model areas basically delineated the large river basins in the continent (Figure 1) and included: Area 1, Niger, Chad, and North Africa with an area of 11.8 million km^2 and 106 stations; Area 2, Nile with an area of 6.1 million km^2 and 27 stations; Area 3, Congo with an area of 4.8 million km^2 and 38 stations; and Area 4, Zambezi, South Africa, and Madagascar with an area of 5.1 million km^2 and 36 stations. The zoning was based on the intracontinental variations in the climate as well as the dominant land covers and soil types.

[19] The choice of the parameters initially included in the calibration procedures was based on the experience gained in modeling West Africa [*Schuol et al.*, 2008] for which a detailed literature-based preselection as well as a sensitivity analysis has been performed. Some of the selected SWAT parameters (e.g., curve number) are closely related to land cover, while some others (e.g., available water capacity, bulk density) are related to soil texture. For these parameters a separate value for each land-cover/soil-texture was selected, which increased the number of calibrated parameters substantially. The percentage of land cover and soil texture distribution within Africa and the four subregions is listed in Table 1. In the course of the iterative SUFI-2 calibration, not only the parameter ranges were narrowed, but also the number of parameters was decreased by excluding those that turned out to be insensitive.

[20] To account for the uncertainty in the measured discharge data, a relative error of 10% [*Butts et al.*, 2004] and an absolute measured discharge uncertainty of 0.1 $m^3\ s^{-1}$ were included when calculating the *P-factor*. The absolute uncertainty was included in order to capture the dry periods of the many intermittent streams.

3. Results and Analysis

3.1. Model Calibration

[21] The three calibration procedures produced more or less similar results for the whole of Africa in terms of the values of the objective function Φ, the *P-factor*, and the *R-factor* (Table 2). The final parameter ranges in the three procedures, although different, were clustered around the same regions of the parameter space as shown in Table 3. This is typical of a nonuniqueness problem in the calibration of hydrologic models. In other words, if there is a single model that fits the measurements there will be many of them [*Abbaspour*, 2005; *Abbaspour et al.*, 2007]. *Yang et al.* [2008] used four different calibration procedures, namely GLUE, MCMC, ParaSol, and SUFI-2, for a watershed in China. All four produced very similar final results in terms of R^2, Nash-Sutcliffe (*NS*), *P-factor* and *R-factor* while converging to quite different final parameter ranges. In this study also, where only SUFI-2 was used with three different objective functions, all three methods resulted in different final parameter values.

Table 2. Final Statistics for the Three Calibration Procedures

	Φ		P-factor		R-factor	
	Cal.	Val.	Cal.	Val.	Cal.	Val.
Procedure 1	0.44	0.47	55.4	55.6	1.56	1.48
Procedure 2	0.44	0.46	58.9	58.5	1.65	1.49
Procedure 3	0.48	0.48	60.8	59.3	1.52	1.43

[22] In the following, we used the results of the third approach, because dividing Africa into four different hydrologic regions accounted for more of the spatial variability and resulted in a slightly better objective function value.

[23] In order to provide an overview of the model performance in different regions, the P-factor (percent data bracketed) and the R-factor (a measure of the thickness of the 95PPU band) at all the stations across Africa are shown for both calibration and validation in Figure 2. In addition, the efficiency criteria, Φ, calculated based on the observed and the "best" simulation (i.e., simulation with the largest value of the objective function), and also the NS coefficient are shown at each station. Overall, in calibration (valida-

tion), at 61% (55%) of the stations over 60% of the observed data were bracketed by the 95PPU and at 69% (70%) of the stations the R-factor was below 1.5. The Φ value was at 38% (37%) of the stations higher than 0.6 and the NS was at 23% (21%) of the stations higher than 0.7. In general, the model performance criteria were quite satisfactory for such a large-scale application. Some areas of poorly simulated runoffs were the Upper Volta, the East African Lakes region, and the Zambezi and Orange basin in the South of Africa. The reasons for this might be manifold and are not always clearly attributable. Of great importance are (1) over- or under-estimation in precipitation; (2) difficulties in simulating the outflow from lakes and wetlands; (3) insufficient data on the management of the reservoirs; (4) the effect of smaller lakes, reservoirs, wetlands, and irrigation projects that were not included; (5) simplifications by using dominant soil types and land cover classes in the subbasins; and (6) various water use abstractions, which were not included.

3.2. Quantification of Blue and Green Water Resources and Their Uncertainty Ranges

[24] Using the calibrated model, the annual and monthly blue water flow (water yield plus deep aquifer recharge),

Table 3. SWAT Model Parameters Included in the Final Calibration Procedures and Their Initial and Final Ranges[a]

Parameter Name	Initial Range	1st Proc. Final Range	2nd Proc. Final Range	3rd Proc. Final Range			
				Area 1	Area 2	Area 3	Area 4
CN2__BSVG*	−0.50–0.15	−0.45–(−0.05)	−0.40–0.00	...	−0.40–(−0.10)	...	...
CN2__CRDY*	−0.50–0.15	−0.25–0.05	−0.05–0.10	−0.45–(−0.10)	...	−0.20–0.15	−0.10–0.10
CN2__FODB*	−0.50–0.15	−0.45–(−0.05)	−0.35–0.00	...	...	−0.30–0.00	−0.45–(−0.05)
CN2__FOEB*	−0.50–0.15	−0.30–0.05	−0.20–0.10	−0.45–0.10	...	−0.25–0.10	...
CN2__GRAS*	−0.50–0.15	−0.40–0.00	−0.35–(−0.05)	−0.38–0.02	...	...	−0.40–(−0.10)
CN2__SAVA*	−0.50–0.15	−0.50–(−0.20)	−0.50–(−0.30)	−0.50–(−0.35)	−0.25–0.00	−0.45–(−0.20)	−0.10–0.15
CN2__SHRB*	−0.50–0.15	−0.45–0.05	−0.35–(−0.10)	...	−0.45–(−0.10)	...	−0.35–0.15
CN2__CRWO*	−0.50–0.15	...	...	0.00–0.17	−0.45–0.05	−0.45–0.15	...
CN2__MIGS*	−0.50–0.15	...	...	−0.40–0.10	...	...	...
CN2__FOMI*	−0.50–0.15	...	...	...	...	−0.45–0.10	...
CN2__CRGR*	−0.50–0.15	...	...	...	...	...	−0.45–0.00
S_AWC__C*	−0.50–0.50	−0.40–0.00	−0.50–(−0.05)	...	−0.25–0.40	−0.48–0.00	−0.20–0.50
S_AWC__CL*	−0.50–0.50	−0.40–0.10	−0.20–0.15	0.00–0.45	−0.45–0.20	−0.25–0.30	−0.45–0.00
S_AWC__L*	−0.50–0.50	−0.25–0.30	0.15–0.50	−0.15–0.40	−0.30–0.15	−0.05–0.20	−0.30–0.10
S_AWC__LS*	−0.50–0.50	−0.50–0.20	−0.30–0.50	...	−0.30–0.25	...	−0.20–0.45
S_AWC__SCL*	−0.50–0.50	−0.35–0.05	−0.20–0.30	−0.10–0.25	−0.50–(−0.20)	−0.40–0.25	−0.35–0.00
S_AWC__SL*	−0.50–0.50	−0.20–0.40	−0.20–0.50	−0.20–0.15	−0.15–0.30	−0.30–0.20	0.00–0.45
S_AWC__S*	−0.50–0.50	...	...	−0.20–0.45	...	...	...
S_BD__C*	−0.50–0.50	−0.40–0.20	−0.25–0.15	...	−0.04–0.23	−0.35–0.10	−0.10–0.40
S_BD__CL*	−0.50–0.50	−0.25–0.40	−0.25–0.20	−0.30–0.30	−0.05–0.10	−0.25–0.45	−0.45–0.30
S_BD__L*	−0.50–0.50	−0.05–0.35	−0.05–0.40	−0.10–0.40	−0.10–0.35	−0.45–0.25	−0.25–0.15
S_BD__LS*	−0.50–0.50	−0.40–0.25	−0.45–(−0.05)	...	...	−0.32–0.10	−0.40–0.35
S_BD__SCL*	−0.50–0.50	−0.15–0.40	−0.20–0.30	−0.35–0.25	−0.45–0.20	−0.45–0.00	−0.35–0.25
S_BD__SL*	−0.50–0.50	−0.30–0.35	−0.20–0.25	−0.25–0.10	−0.20–0.40	−0.45–0.25	−0.10–0.45
S_BD__S*	−0.50–0.50	...	...	−0.40–0.20	...	...	...
ESCO	0.00–1.00	0.10–0.60	0.35–0.70	0.25–0.55	0.10–0.50	0.20–0.65	0.10–0.60
GW_DELAY	0–100	1–30	20–40	25–42	0–30	30–60	10–80
GW_REVAP	0.02–0.20	0.03–0.17	0.08–0.16	0.05–0.13	0.02–0.13	0.02–0.09	0.03–0.17
GWQMN	0–1000	20–300	25–300	175–350	200–750	125–400	5–100
RCHRG_DP	0.00–1.00	0.35–0.65	0.35–0.60	0.40–0.55	0.25–0.65	0.25–0.50	0.10–0.55
REVAPMN	0–500	225–500	200–500	275–500	200–400	225–375	125–350
SURLAG	0.0–10.0	2.0–8.0	2.0–4.5	...	...	...	...

[a]CN2, SCS runoff curve number; S_AWC, soil available water storage capacity; S_BD, moist soil bulk density; ESCO, soil evaporation compensation factor [−]; GW_DELAY, groundwater delay time (lag between the time that water exits the soil profile and enters the shallow aquifer) [days]; GW_REVAP, groundwater 'revap' coefficient (regulates the movement of water from the shallow aquifer to the root zone [−]; GWQMN, threshold depth of water in the shallow aquifer required for return flow [mm H$_2$O]; RCHRG_DP, deep aquifer percolation fraction [−]; REVAPMN, threshold depth of water in the shallow aquifer for 'revap' or percolation to the deep aquifer [mm H$_2$O]; SURLAG, surface runoff lag coefficient [days] CN2, S_AWC and S_BD have different parameter values depending on the land cover or the soil texture type. For the abbreviations please refer to Table 1. Asterisk means relative change of the parameter value.
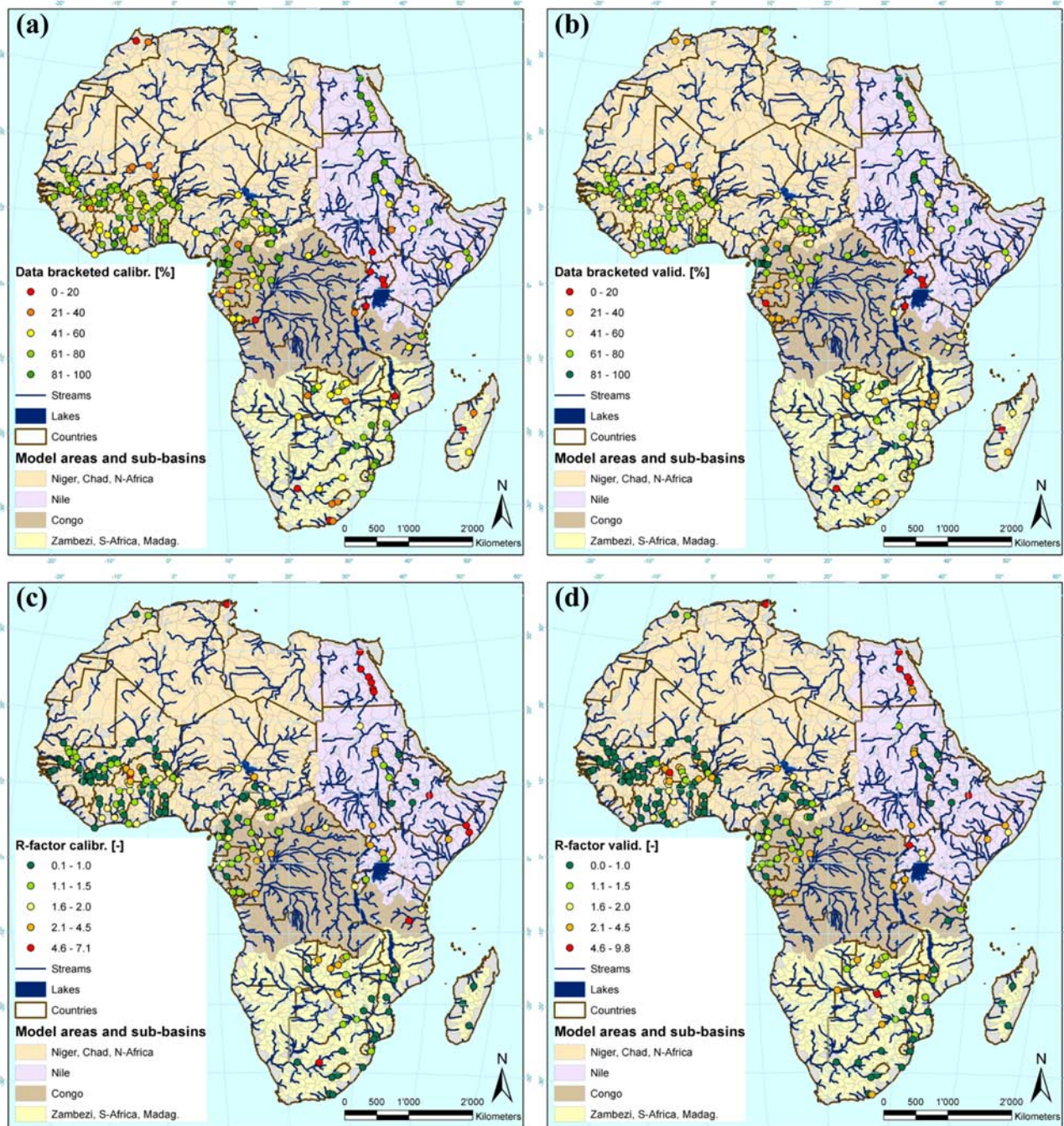
Figure 2. The *P-factor* (a, b), the *R-factor* (c,d), the weighted coefficient of determination Φ (e, f), and the Nash-Sutcliff coefficient (g, h) of the calibration (a, c, e, g) and validation (b, d, f, h) at all 207 stations.

green water flow (actual evapotranspiration), and green water storage (soil water) were calculated for each subbasin and summed up for different countries or regions and also the whole continent. We compared our model results with other studies for blue water flow only, as to the best of our knowledge, the green water flow and storage were not explicitly quantified in the other models. Figure 3 shows the estimated annual blue water for the whole African continent averaged over the period 1971–1995 and the results of ten other existing data-based (DB) or model-based (M) assessments. A direct one-to-one comparison of these

values is not possible due to the different time periods and study-specific assumptions. The intent of this comparison is to give an overview of the differences in the existing numbers that are used in various advanced studies. The variation in different estimates indicates the uncertainty associated in such calculations, which is captured almost entirely in our prediction uncertainty as shown in Figure 3.

[25] On the country basis, the simulated long-term annual (averaged over 1971–1995) blue water flow availability in mm a^{-1} was compared with two other global assessments: the FAO estimates [*FAO*, 2003] and the annual (averaged
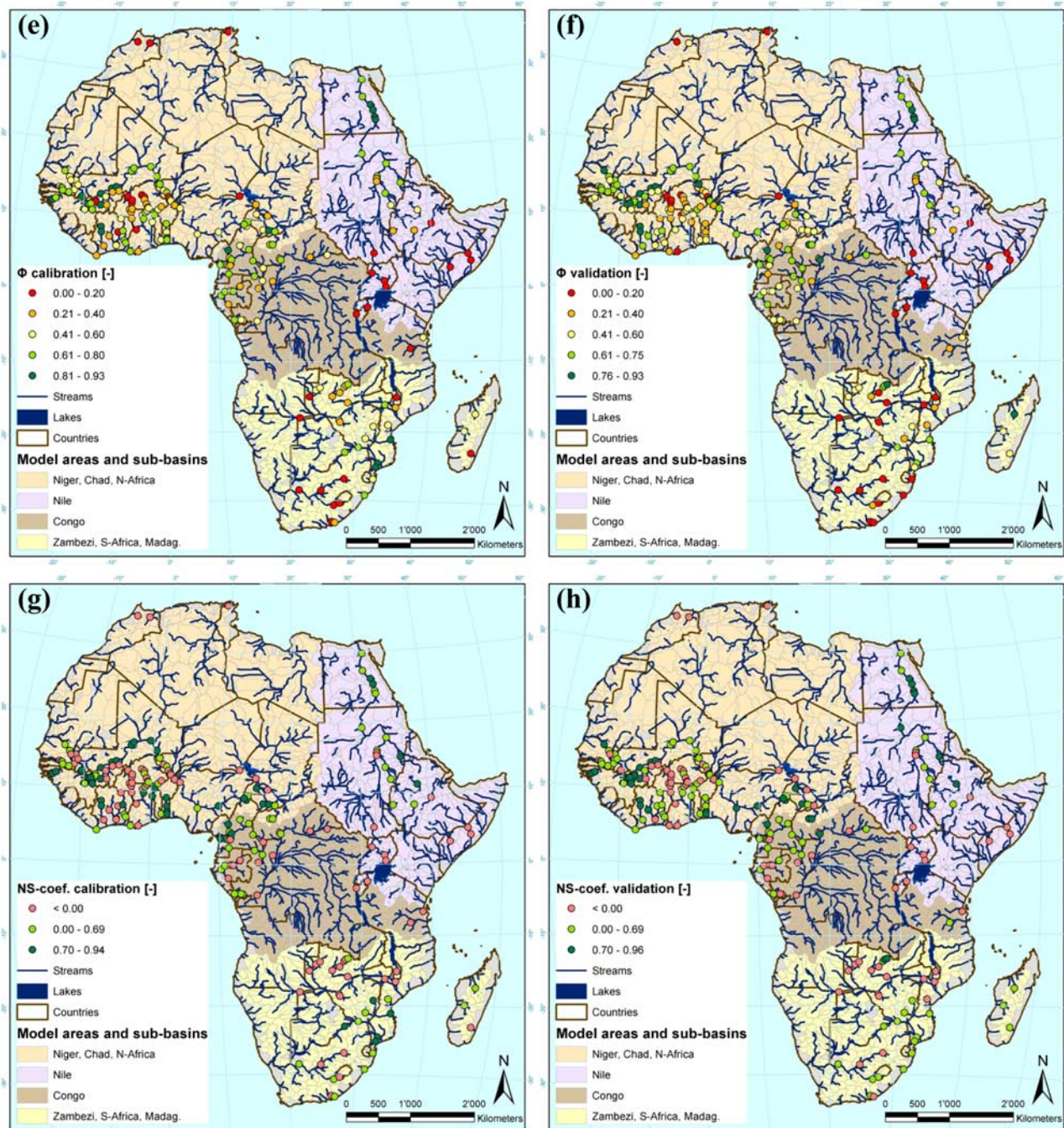
Figure 2. (continued)

over 1961–1995) simulation from WaterGAP 2.1e model (Figure 4). The latter has been produced for the 2005 Environmental Sustainability Index calculation [*Esty et al.*, 2005]. For the sake of clarity in illustration, the very high FAO values for Liberia (2077 mm a^{-1}) and Sierra Leone (2206 mm a^{-1}) were not included in the figure (limited y axis range). Also not shown in the figure are the values for six African countries for which WaterGAP produced negative values (as it considers evaporation losses from lakes and wetlands even though they depend on inflow from other countries). In general, the large differences between FAO and WaterGAP estimates indicate the uncer-

tainty in the country-based blue water estimates. Overall, a large number of these estimates fell within our prediction uncertainties. Although the calculated uncertainties may appear large, we maintain that the actual uncertainty may indeed be even larger because the coverage of the measured data in the 95PPU was in some areas relatively small (small *P-factor*). To decrease model uncertainty, a better description of the climate data, reservoir management, and water use would be essential.

[26] In Table 4 the annual average water availability in each country is shown in km^3 a^{-1}. The subbasin-based precipitation and the 95PPU ranges for the blue water flow,
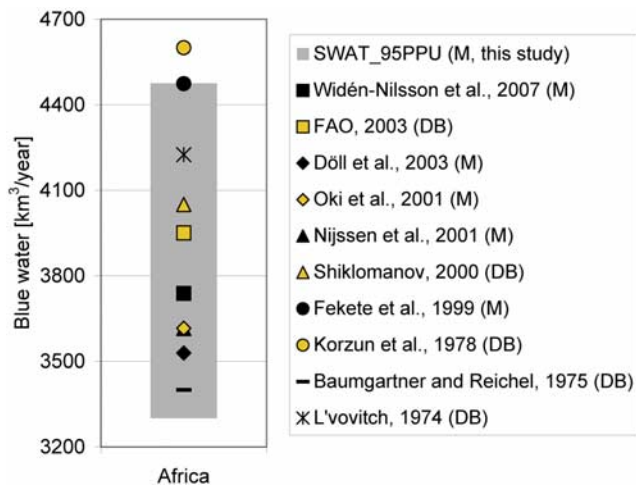
Figure 3. The SWAT 95PPU range of the 1971 to 1995 annual average blue water flow availability for the African continent compared with 10 other existing assessments.

green water flow, and the green water storage were aggregated to obtain country- and then continental-based values. The uncertainties (95PPU) in green water flow estimates were generally smaller than those of the blue water flow or green water storage because of its sensitivity to fewer parameters. It should be noted that the modeled green water storage was solely calibrated indirectly as there were no soil moisture observations. This study explored the possibility

of using data from remote sensing satellites, but so far only found monitored surface soil moisture (top few centimeters) in areas without forest or sand dunes. The relationship between these values and that of the root zone soil moisture is still unclear [*Wagner et al.*, 2003, 2007].

[27] Next to the above annual continental and country-based estimates, this study also provides monthly time series of freshwater components for each subbasin with valuable information on both spatial and temporal distributions. Such information has not been available at this detail for the whole continent. In Figures 5a–5c the long-term average annual freshwater components are shown in each subbasin. These figures show the local (subcountry) differences especially in large countries with partly (semi-)arid climate. In areas like North Africa, the south of Chad (Chari basin), or the Limpopo basin in the South-East of Africa, with scarce blue water availability, there are considerable green water resources sustaining ecosystems, rain-fed agriculture and ultimately people's lives.

[28] Despite the spatial distribution, the intra- and inter-annual variability of the freshwater availability is of great importance. Figure 6 shows the coefficient of variation (CV) of the 1971–1995 annual values in each subbasin for the blue water flow, the green water flow and the green water storage. In general the CV, which is an indicator for the reliability of a freshwater source, varied noticeably within the continent and was the lowest for the green water flow, while it was the largest for the blue water flow. The reason for this is that the supply of water for evapotranspiration is limited by soil's capacity to deliver water to the
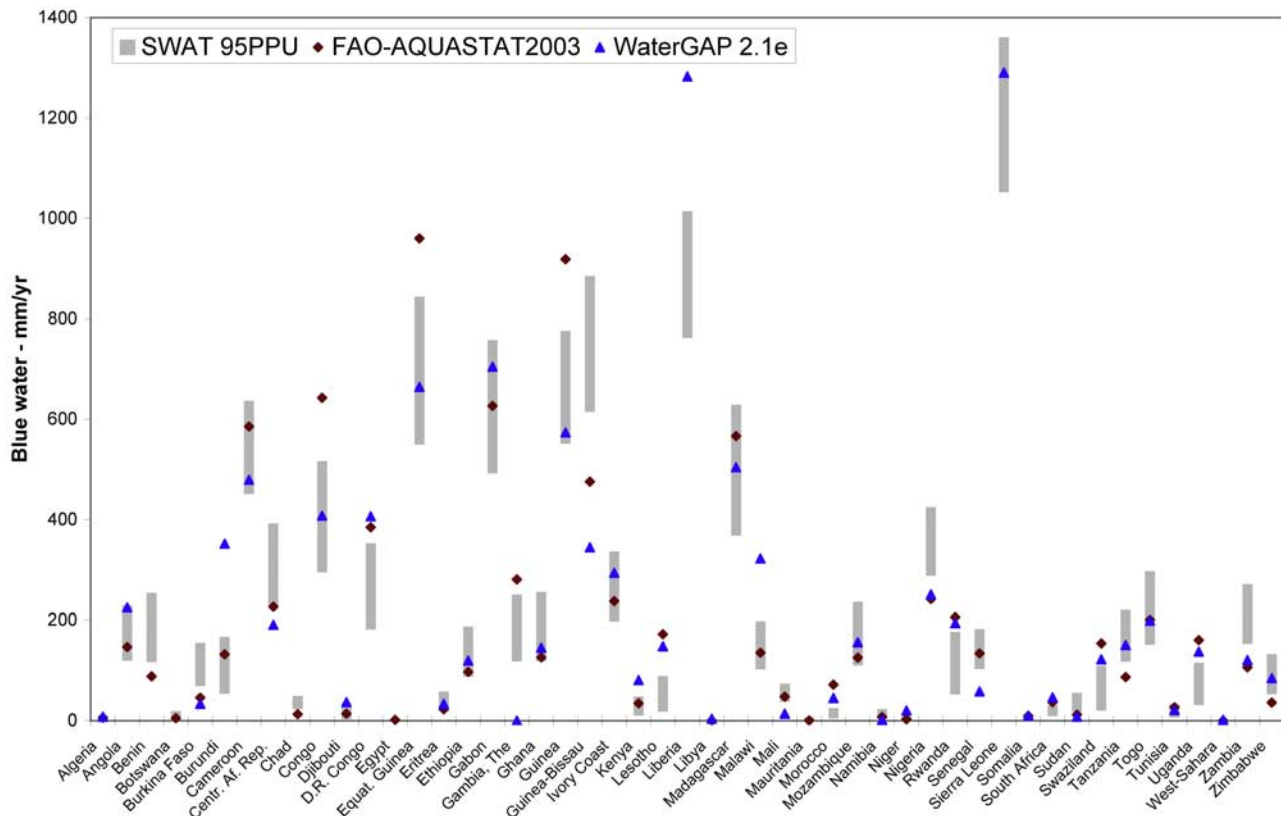

Figure 4. Comparison of the SWAT 95PPU ranges of the annual average (1971–1995) blue water flow availability in the African countries with the results from the FAO assessment and the WaterGAP model.

Table 4. Average Precipitation (Model Input) and the 95PPU Ranges for the Components of Freshwater Availability in the African Countries

Country	Area, 10^3 km^2	Precipitation, km^3 a^{-1}	Blue Water Flow, km^3 a^{-1}	Green Water Flow, km^3 a^{-1}	Green Water Storage, km^3
Algeria	2321.0	198.6	2.1–8.8	181.5–200.1	9.8–13.8
Angola	1252.4	1232.3	150.0–287.3	893.8–1024.1	49.4–71.1
Benin	116.5	116.4	13.7–29.6	84.6–96.1	4.4–6.8
Botswana	580.0	226.9	2.4–11.1	201.5–234.2	6.9–13.5
Burkina Faso	273.7	201.3	19.0–42.5	153.1–173.1	6.6–10.0
Burundi	27.3	32.3	1.5–4.5	22.2–24.6	1.2–2.1
Cameroon	466.3	751.8	210.5–296.9	443.0–492.0	23.9–36.4
Cent. Af. Rep.	621.5	809.8	143.2–243.8	545.4–615.5	29.6–42.8
Chad	1168.0	397.3	26.9–57.6	325.8–363.2	16.7–24.0
Congo	345.4	554.5	102.1–178.5	361.0–411.1	19.3–30.0
D.R. Congo	2337.0	3526.9	424.8–825.2	2525.9–2841.9	160.7–255.9
Djibouti	21.6	6.1	0.1–0.8	4.8–6.3	0.1–0.2
Egypt	982.9	36.3	0.0–0.3	34.8–37.1	0.5–0.7
Equat. Guinea	27.1	52.9	14.9–22.9	29.4–33.4	1.5–2.8
Eritrea	121.9	38.1	2.3–7.1	29.1–33.9	0.6–1.3
Ethiopia	1132.3	877.5	99.1–211.9	627.7–707.2	19.9–38.4
Gabon	261.7	462.6	128.8–198.3	257.4–295.4	12.5–21.8
Gambia, The	10.7	8.2	1.3–2.7	5.4–6.3	0.2–0.4
Ghana	240.0	277.6	28.5–61.4	208.2–234.8	9.7–16.3
Guinea	246.1	398.6	135.7–190.9	210.6–234.3	12.8–18.9
Guinea-Bissau	33.6	50.4	20.7–29.8	22.0–25.0	1.4–2.0
Ivory Coast	322.2	418.5	63.6–108.5	301.1–332.7	16.1–24.2
Kenya	584.4	383.8	6.0–28.3	308.4–331.6	9.7–15.2
Lesotho	30.4	22.0	0.6–2.7	18.3–21.2	0.6–1.4
Liberia	96.3	213.7	73.4–97.7	115.9–125.1	6.3–9.0
Libya	1620.5	76.6	0.1–0.7	72.1–79.7	2.6–3.8
Madagascar	594.9	864.4	219.1–374.2	502.8–566.4	32.8–57.8
Malawi	119.0	130.9	12.2–23.5	51.2–58.0	1.5–2.6
Mali	1256.7	366.3	47.7–92.1	267.7–297.8	8.5–12.6
Mauritania	1041.6	89.9	2.3–7.2	78.7–87.4	1.0–1.7
Morocco	403.9	113.6	1.9–10.2	98.0–113.2	6.4–9.4
Mozambique	788.6	769.5	87.1–186.6	522.1–630.0	25.8–47.8
Namibia	825.6	237.6	3.0–19.0	204.5–243.4	6.3–13.2
Niger	1186.0	185.3	3.3–9.4	165.5–186.6	5.3–8.8
Nigeria	912.0	1004.0	263.1–387.6	605.2–677.2	35.2–49.6
Rwanda	25.2	30.1	1.3–4.5	25.0–27.3	1.4–2.5
Senegal	196.9	124.1	20.4–35.9	85.3–97.4	3.6–5.7
Sierra Leone	72.5	166.5	76.3–98.7	70.0–76.8	4.1–6.0
Somalia	639.1	190.6	1.2–7.8	174.5–190.8	4.6–7.3
South Africa	1223.1	578.8	11.3–37.4	521.7–568.9	16.6–29.7
Sudan	2490.4	1020.7	45.1–138.3	830.9–930.7	28.3–44.4
Swaziland	17.2	14.5	0.4–1.9	11.8–14.0	0.3–0.9
Tanzania	945.0	977.5	111.4–208.3	599.3–666.4	24.0–35.0
Togo	57.3	63.8	8.7–17.0	45.8–51.0	2.2–3.3
Tunisia	155.4	44.7	1.0–5.1	37.3–44.2	2.7–4.3
Uganda	243.0	283.6	7.7–28.0	206.9–228.1	6.7–14.1
W. Sahara	269.6	9.3	0.0–0.0	8.7–9.7	0.1–0.2
Zambia	754.8	727.5	115.6–204.9	479.5–559.8	25.1–38.8
Zimbabwe	390.8	256.0	20.7–51.7	193.9–234.5	8.4–16.0
Africa	30222	19865	3301–4476	14449–15348	785–996

roots. This capacity is within a narrow range between soil's field capacity and wilting point. The interannual variability of the blue water flow is especially large in the Sahel, at the Horn of Africa, and in the Southern part of Africa, areas which are known for recurring severe droughts.

[29] The intra-annual variability, presented by the 1971–1995 average monthly 95PPU bands of the blue water flow, the green water flow and the green water storage is shown in Figure 7 for three countries as an example. These countries, all with different climatic conditions, are Niger in Western Africa, Zimbabwe in the Southern Africa, and Gabon in Central Africa with an annual average precipitation of 185 mm, 256 mm, and 463 mm, respectively. In order to see the relation between the freshwater components and the water input, the figures also include the average monthly precipitation. All values are shown in mm or mm month^{-1} and thus can be directly compared. The trends in blue water flow in different countries become clearly apparent. Niger and Zimbabwe, in particular, show large uncertainties for the wet months. It should be noted that the reported uncertainties in the average monthly values combine both modeling uncertainties as well as natural variability. Hence the reliability of the water resources decreases as the uncertainties increase. The green water storage can potentially benefit the agriculture in months with little or without precipitation. In Niger the soil water storage is depleted for about half of the year, while in Gabon this volume persists much longer within the (much shorter) dry
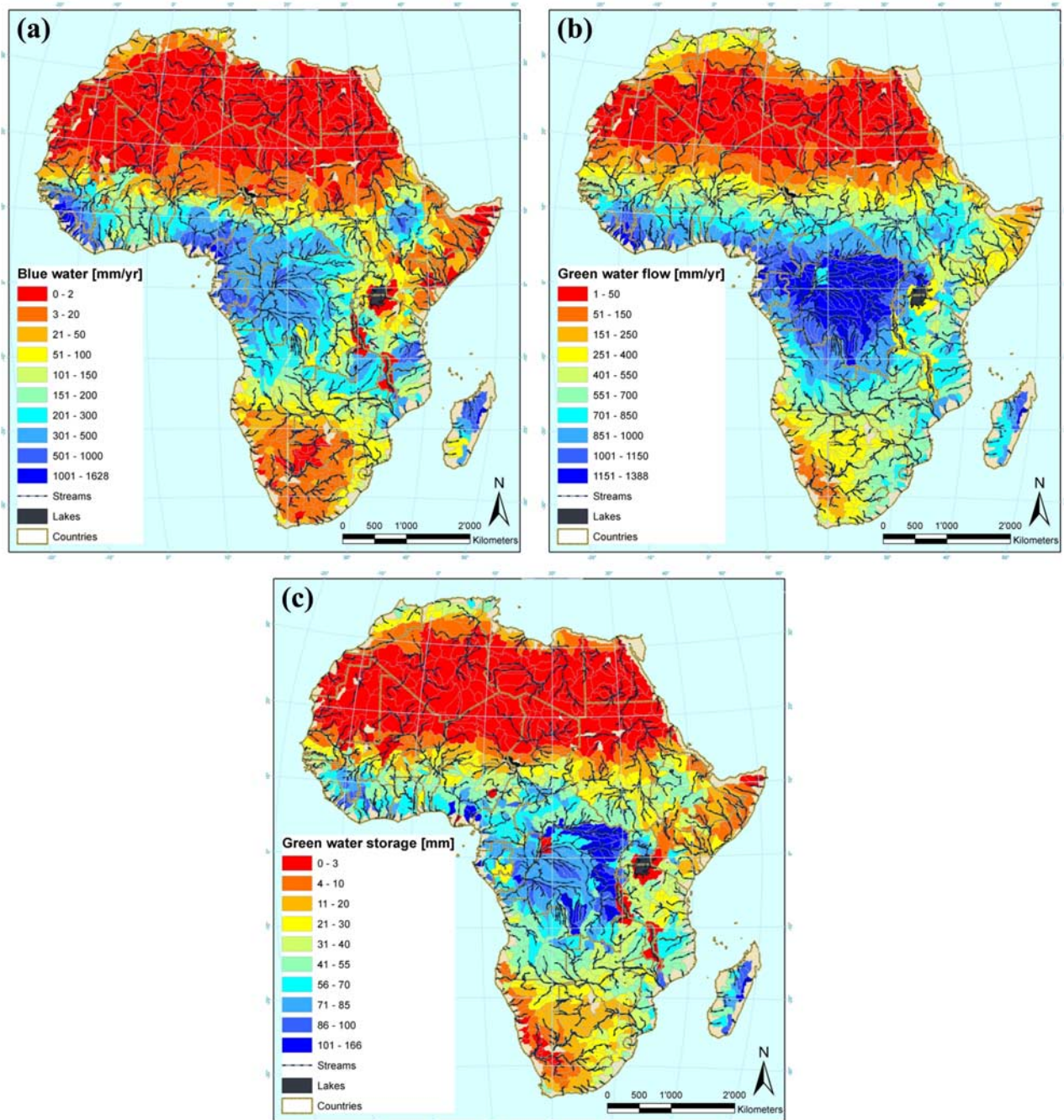
Figure 5. The 1971 to 1995 annual average (a) blue water flow, (b) green water flow, and (c) green water storage in all 1496 modeled subbasins in Africa.

period. This information is quite helpful in planning cropping season and helps to model scenarios of changing cropping seasons and patterns and its impacts on green and blue water flow and storage.

[30] It should be pointed out that for large countries, variations can be substantial across subbasins. For example, in Niger the country-based annual average blue water flow availability is 3 to 8 mm a^{-1} but some subbasins in the south of the country provide about 10 times more. While not shown in further detail, the model can provide monthly information of the freshwater components for each of the

1496 subbasins in Africa and they will be published in a special report.

4. Implications of the Model Results

4.1. Blue Water Scarcity Indicators Considering Uncertainty

[31] The model results of the temporal and spatial variations of the freshwater availability components and their uncertainty bands can be used in global and national water planning and management, in advanced studies concerning
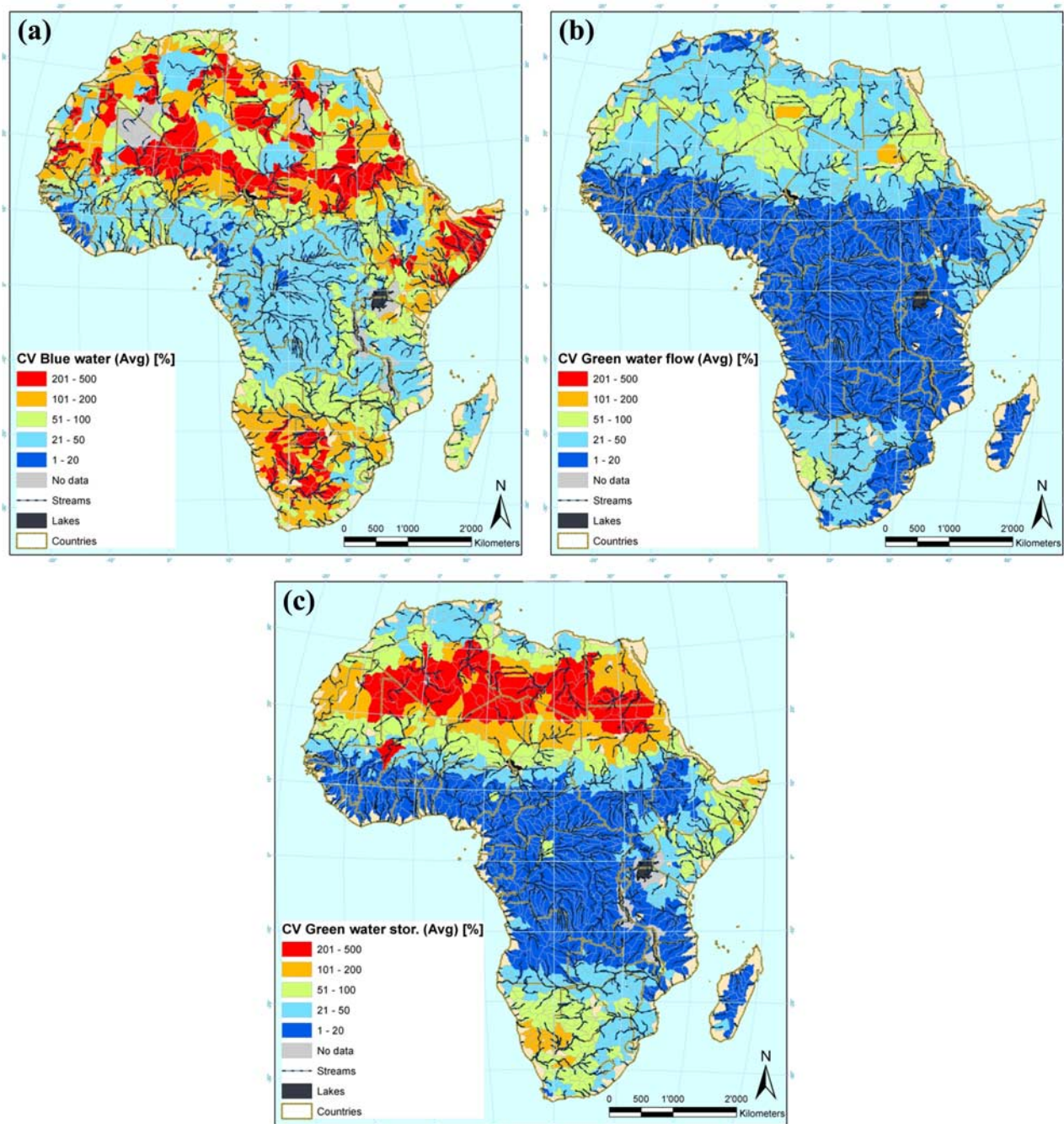
Figure 6. Coefficient of variation (CV) of the average of the 95PPU ranges (Avg.) of the 1971 to 1995 modeled annual values of the (a) blue water flow, (b) green water flow, and (c) green water storage in each subbasin.

the water and food security, virtual water flow, and effects of land-use and climate change [*UNESCO*, 2006]. This study briefly presents the use of the model results for water scarcity analysis. While there exist a large number of water scarcity indicators, one of the most widely used and accepted is the water stress threshold, defined as 1700 m^3 capita^{-1} a^{-1} [*Falkenmark and Widstrand*, 1992]. This scarcity index does not indicate that water is scarce for domestic purposes, but rather for irrigation and thus for food production [*Rijsberman*, 2006]. *Yang et al.* [2003]

have found that below a threshold of about 1500 m^3 capita^{-1} a^{-1} the cereal import in a country inversely correlates to its renewable water resources. Below this value different degrees of water stresses (extreme stress: <500 m^3 capita^{-1} a^{-1}, high stress: <1000 m^3 capita^{-1} a^{-1}) can be defined [*Falkenmark et al.*, 1989]. A value between 1700 and 4000 m^3 capita^{-1} a^{-1} is considered as just adequate [*Revenga et al.*, 2000]. *Vörösmarty et al.* [2000] have found in a global study that the number of people exposed to high water stress (defined as withdrawal-to-availability-ratio
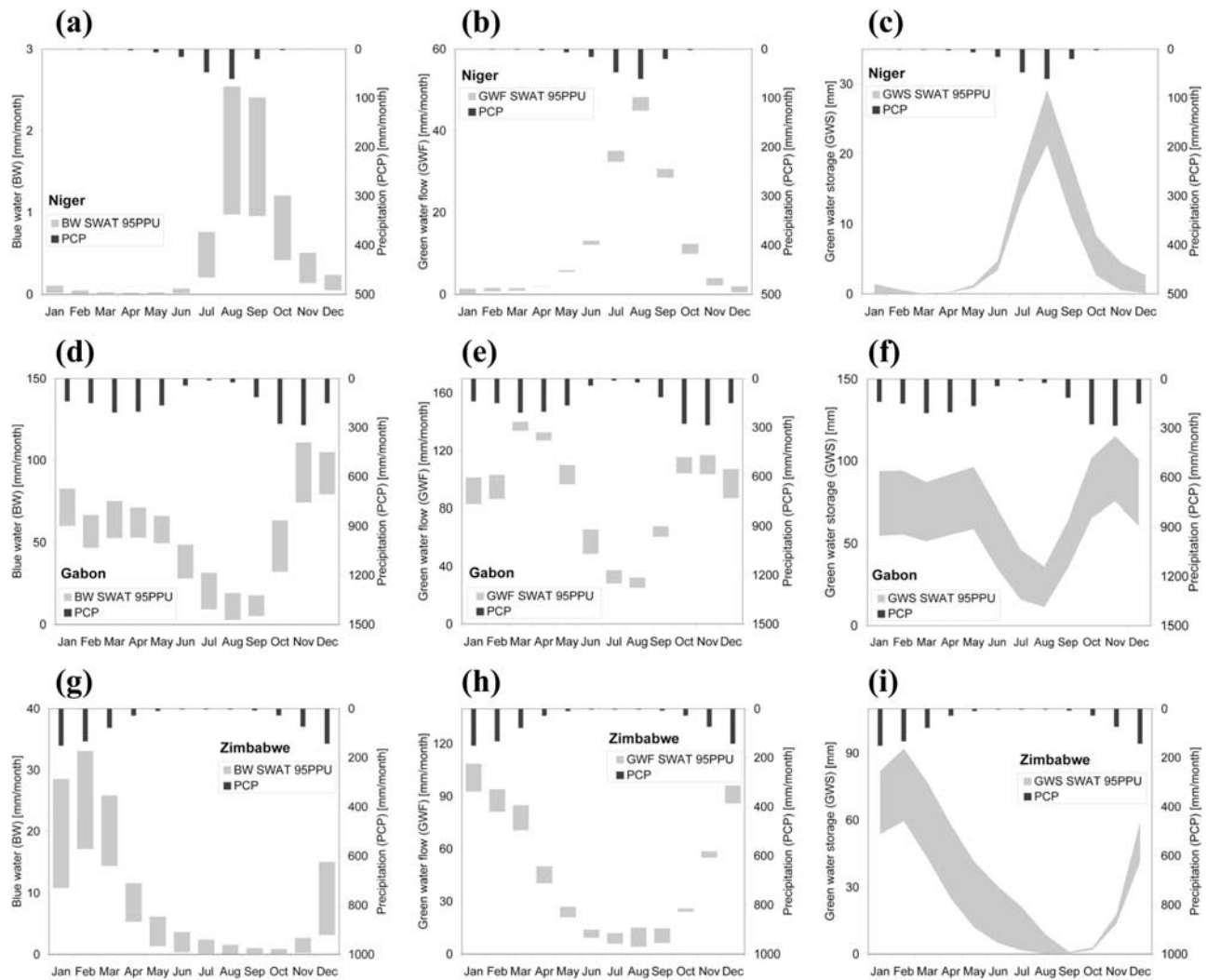
Figure 7. Average (1971–1995) monthly 95PPU ranges of (a, d, g) the blue water flow, (b, e, h) the green water flow, and (c, f, i) the green water storage in the countries Niger (Figures 7a–7c), Gabon (Figures 7d–7f), and Zimbabwe (Figures 7g–7i).

larger than 0.4) is three times larger if the analysis is based on geospatial data at a resolution of 50 km instead of using national estimates. According to *Rijsberman* [2006] one of the limitations of water scarcity indicators are the annual, national averages that hide important scarcity at monthly and regional scales.

[32] We computed the water availability per capita and water stress indicators not only for each country but also for each of the 1496 subbasins. The population estimates were taken from the Center for International Earth Science Information Network's (CIESIN) Gridded Population of the World (GPW, version 3, http://sedac.ciesin.columbia. edu/gpw). The data are for the year 2005 and has a spatial resolution of 2.5 arc-min, which we aggregated for each subbasin. In order to address uncertainty of future water stress estimates, *Alcamo et al.* [2007] computed and compared globally three different indicators of water stress (withdrawals-to availability ratio greater than 0.4, water availability per capita less than 1000 m^3 a^{-1}, and consumption-to-Q90 ratio greater than 1). Although there was a large overlap in the estimated areas with severe water stress, in many regions the three indicators disagreed. Overall, using the water availability per capita indicator resulted in the lowest values of affected area and number of people with severe water stress. In this study we address uncertainty by calculating the per capita water availability by using the lower (L95PPU), the upper (U95PPU) and the average (Avg) 95PPU values of the blue water flow during the simulation time period.

[33] Looking at the water scarcity on a country basis, the use of the L95PPU blue water flow values led to 29 countries with water stress (<1700 m^3 capita^{-1} a^{-1}), while the use of the U95PPU values led to merely 16 affected countries (Table 5). Taking the average of the 95PPU range resulted in 20 vulnerable countries. In countries where both L95PPU and U95PPU result in the same conclusion, the risk situation is quite clear. However, in countries such as Burkina Faso, Ethiopia, Ghana, Sudan, and Zimbabwe where only the use of the L95PPU blue water flow values signalizes water scarcity, the situation demands more detailed studies. One can conclude that in many of these countries, and in fact in larger countries in general, it might

Table 5. Country-Based Per Capita Blue Water Flow (BW) Availability Considering the L95PPU and the U95PPU Value of the Annual Average (1971–1995) BW and the Population in the Year 2005

Country	BW-L95PPU, m³/cap/a	BW-U95PPU, m³/cap/a	Country	BW-L95PPU, m³/cap/a	BW-U95PPU, m³/cap/a
Algeria	63	268	Libya	23	113
Angola	9407	18022	Madagascar	11778	20114
Benin	1619	3508	Malawi	948	1823
Botswana	1336	6297	Mali	3529	6817
Burkina Faso	1440	3210	Mauritania	733	2359
Burundi	194	602	Morocco	60	323
Cameroon	12895	18189	Mozambique	4400	9429
Cent. Af. Rep.	35471	60388	Namibia	1497	9369
Chad	2763	5906	Niger	236	674
Congo	25528	44629	Nigeria	2001	2947
D.R. Congo	7381	14339	Rwanda	147	493
Djibouti	85	955	Senegal	1749	3076
Egypt	1	4	Sierra Leone	13815	17864
Equat. Guinea	29537	45367	Somalia	142	954
Eritrea	530	1614	South Africa	239	789
Ethiopia	1280	2737	Sudan	1245	3816
Gabon	93095	143289	Swaziland	345	1820
Gambia, The	833	1766	Tanzania	2907	5433
Ghana	1290	2776	Togo	1411	2770
Guinea	14438	20308	Tunisia	98	507
Guinea-Bissau	13052	18774	Uganda	266	972
Ivory Coast	3504	5976	W. Sahara	11	91
Kenya	176	825	Zambia	9912	17565
Lesotho	307	1507	Zimbabwe	1591	3974
Liberia	22363	29754	**Africa**	**3613**	**4899**

Underlined cells indicate water stress (< 1700 m³ cap⁻¹ a⁻¹). The shading of the country name cells correspond to the estimated water stress based on the average 95PPU value of the blue water flow availability.

be of great importance to analyze the water scarcity in a spatially distributed manner on a subcountry level rather than consider the country as a whole.

[34] The computed blue water flow availability per capita in each of the 1496 subbasins considering the extremities of the 95PPU range is shown in Figure 8. In critical regions like the Sahel, the South and the East of Africa, the use of the L95PPU and the U95PPU, respectively, lead to quite different assessments of the water scarcity-affected regions and ultimately to the number of the affected people living there.

4.2. Model-Based Uncertainty and Natural Variation in Green Water Storage

[35] Irrigation, water transfer, and virtual water transfer on a regional, national, and international level are common measures to deal with regional blue water scarcity. A better use of the green water, through a more efficient rainfed production, can also partially overcome regional water short falls in countries like Nigeria or South Africa. For the rainfed agriculture, the average (1971–1995) number of months per year where soil water is available (defined as >1 mm m⁻¹) is of utmost importance. This is presented on a subbasin level in Figures 9a and 9b. Because of the model-inherent uncertainties and natural variability, the border of the areas where rainfed agriculture can be realized can shift remarkably. The standard deviation (SD) of the months per year without depleted green water storage is shown for the 1971–1995 period in Figures 9c and 9d. The areas with a high SD (e.g., the Sahel regions in Chad and Niger, Horn of Africa, South of Africa) indicate unreliable green water storage availability which often leads to reduced crop yield

and thus potentially to frequent famines. These areas must develop irrigation systems or alternative cropping practices for a sustainable agriculture.

5. Summary and Conclusion

[36] In this study the well-established semidistributed model SWAT, in combination with the GIS interface ArcS-WAT and SUFI-2 calibration procedure, was successfully applied to quantify the freshwater availability for the whole African continent at a detailed subbasin level and monthly basis with uncertainty analysis. Only globally readily available data sets and information were used for the model setup as well as the model calibration and validation. Within the multisite and multivariable SUFI-2 parameter optimization and uncertainty analysis procedure, three different approaches were performed, which provided valuable insight into the effect of the calibration procedure on model results. The final model results for the freshwater availability components, blue water flow, green water flow, and green water storage were presented at different spatial (continent, countries, and subbasins) and temporal (annual and monthly) resolutions. Particular attention was paid to clearly quantify and display the 95% prediction uncertainty of the outputs, which turned out to be quite large in some cases. The effect of considering these uncertainty estimates in advanced studies was shown for the computation of water scarcity indicators for each of the 1496 subbasins.

[37] Many of the difficulties and limitations within this continental modeling study were data related and resulted from, among others, (1) limited and unevenly distributed rain gauges and discharge stations with varying time series
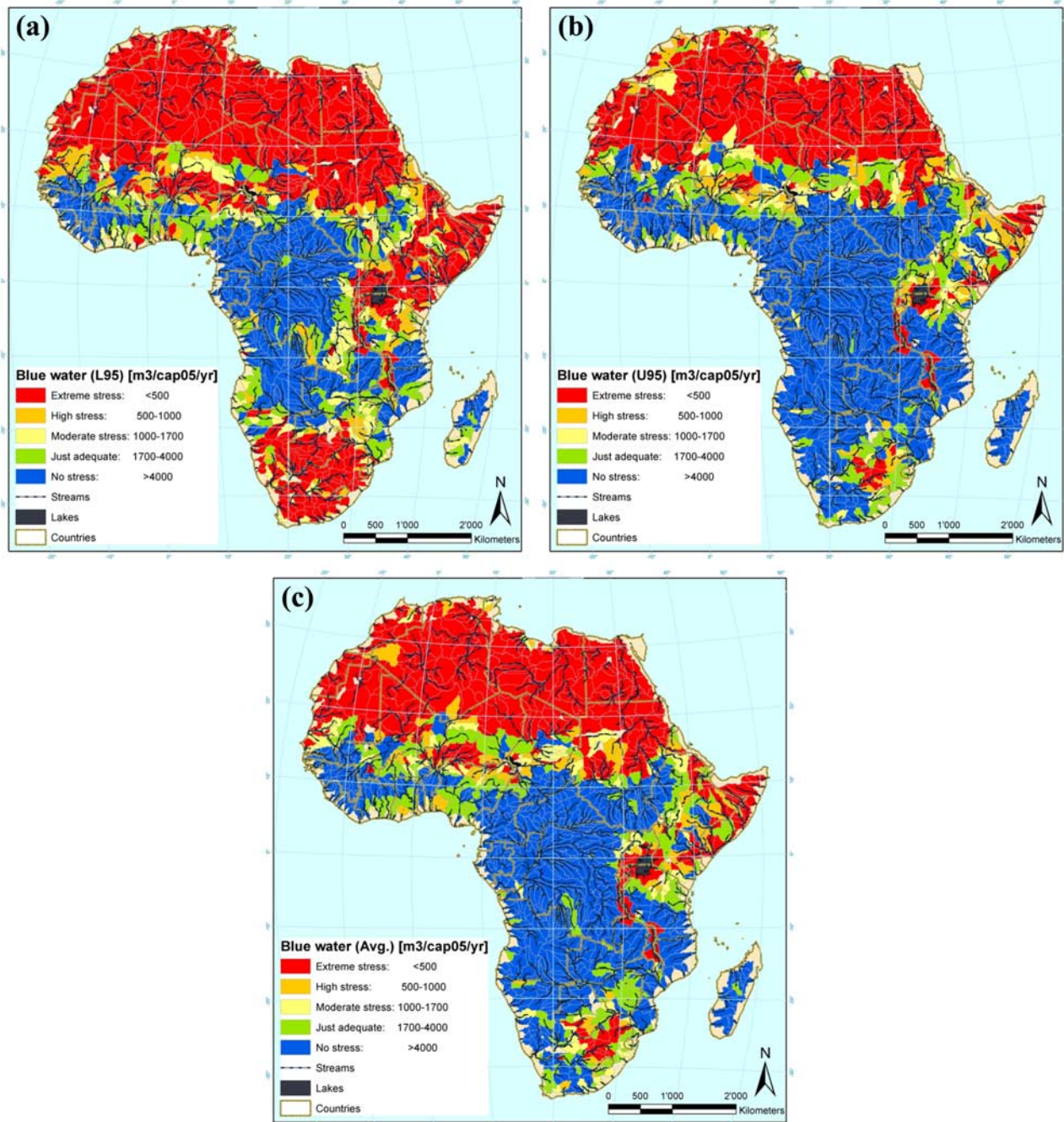
Figure 8. Water scarcity in each modeled African subbasin represented by the modeled 1971 to 1995 annual average blue water flow availability per capita (using population of 2005) using (a) the lower (L95), (b) the upper (U95), and (c) the average (Avg.) value of the 95PPU range.

lengths, (2) limited globally available knowledge of the attributes and especially the management of the reservoirs, and (3) lack of data on soil moisture and/or deep aquifer percolation, which made a desirable calibration/validation of these components impossible. Technical modeling problems in need of further research and improvement were related to the inclusion of the lakes and their outflow to rivers. These resulted in poorer model results in the area of the great lakes of East Africa. This study did not include water use and especially irrigation in the model. Compared

to other continents like Asia, this was thought to be of lesser importance in this study.

[38] Some interesting further development would be to (1) make use of the model results in advanced studies on climate change, water and food security, as well as virtual water trade, which, as it has been pointed out by *Yang and Zehnder* [2007], are in great need of the estimates of spatially and temporally differentiated freshwater components; (2) further improve the African model as new data becomes available (e.g., remote sensing data); and (3) model
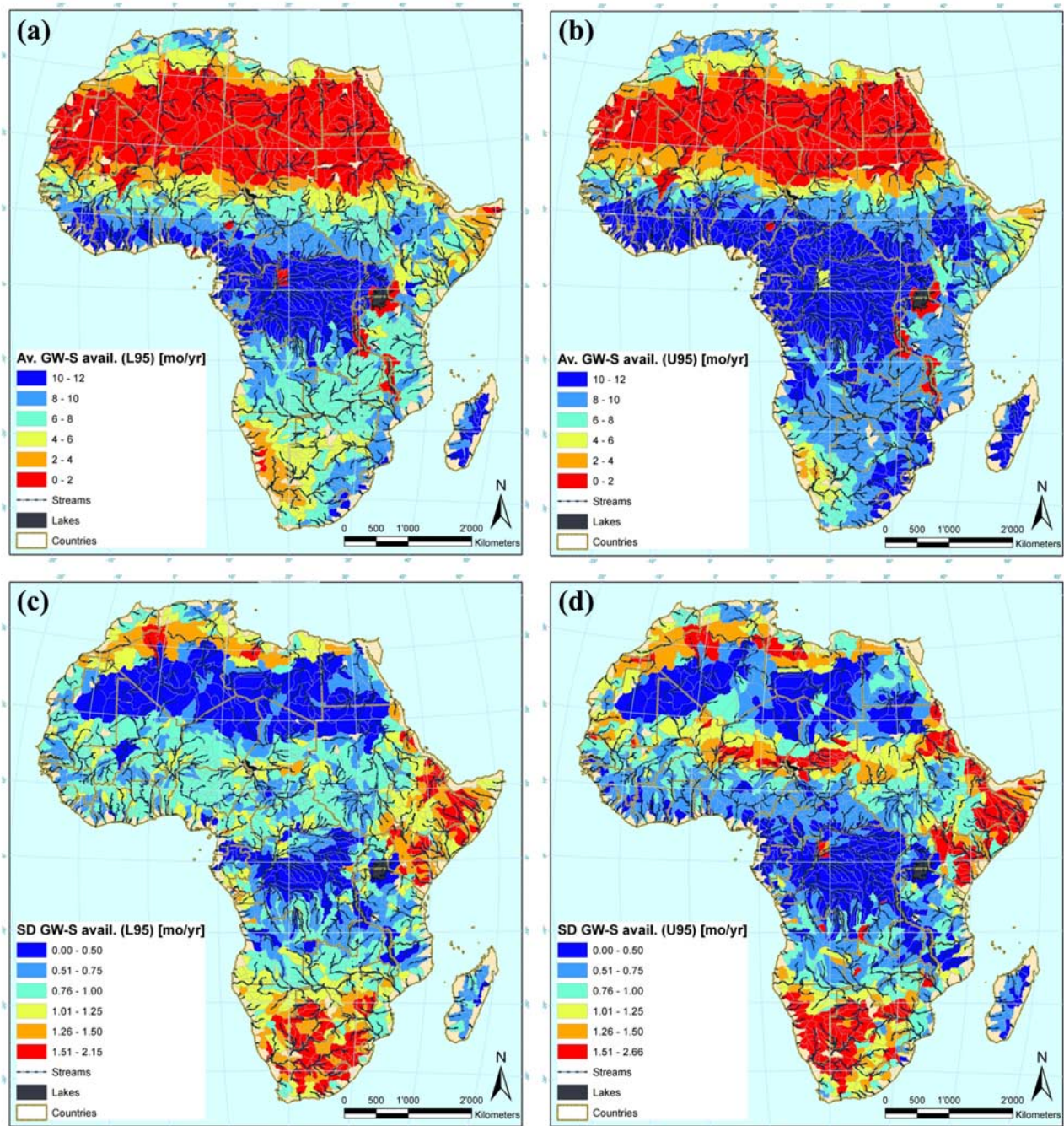
Figure 9. (a, b) The 1971–1995 average (Av.) and (c, d) standard deviation (SD) of the number of months per year where the green water storage (GW-S) is not depleted using the lower (L95) and the upper (U95) value of the 95PPU range.

the freshwater availability in the other continents, in order to finally obtain a global picture.

[39] Overall, this study provided significant insights into continental freshwater availability on a subbasin level and with a monthly time step. This information was very useful for developing an overview of the actual water resources status and helped to spot regions where an in-depth analysis may be necessary. As shown, the inherent uncertainties need to be considered, before general conclusions are drawn.

References

Abbaspour, K. C. (2005), Calibration of hydrologic models: When is a model calibrated?, in *MODSIM 2005 International Congress on Modelling and Simulation*, edited by A. Zerger and R. M. Argent, pp. 2449–2455, Modelling and Stimulation Society of Australia and New Zealand.

Abbaspour, K. C., J. Yang, I. Maximov, R. Siber, K. Bogner, J. Mieleitner, J. Zobrist, and R. Srinivasan (2007), Modelling hydrology and water quality in the pre-alpine/alpine Thur watershed using SWAT, *J. Hydrol.*, *333*, 413–430.

Abbaspour, K. C., J. Yang, M. Vejdani, and S. Haghighat (2008), SWAT-CUP: Calibration and uncertainty programs for SWAT, *4th Int. SWAT Conf. Proc.*, in press.

Alcamo, J., P. Döll, T. Henrichs, F. Kaspar, B. Lehner, T. Rosch, and S. Siebert (2003), Development and testing of the WaterGAP 2 global model of water use and availability, *Hydrol. Sci. J.*, 48(3), 317–337.

Alcamo, J., M. Flörke, and M. Märker (2007), Future long-term changes in global water resources driven by socio-economic and climatic changes, *Hydrol. Sci. J.*, 52(2), 247–275.

Arnell, N. W. (1999), Climate change and global water resources, *Global Environ. Change*, 9, S31–S49.

Arnold, J. G., R. Srinivasan, R. S. Muttiah, and J. R. Williams (1998), Large area hydrologic modeling and assessment. Part I: Model development, *J. Am. Water Resour. Assoc.*, 34(1), 73–89.

Arnold, J. G., R. Srinivasan, R. S. Muttiah, and P. M. Allen (1999), Continental scale simulation of the hydrologic balance, *J. Am. Water Resour. Assoc.*, 35(5), 1037–1051.

Baumgartner, A., and E. Reichel (1975), *The World Water Balance*, 182 pp., Elsevier, New York.

Beven, K., and A. Binley (1992), The future of distributed models - Model calibration and uncertainty prediction, *Hydrol. Processes*, 6(3), 279–298.

Butts, M. B., J. T. Payne, M. Kristensen, and H. Madsen (2004), An evaluation of the impact of model structure on hydrological modelling uncertainty for streamflow simulation, *J. Hydrol.*, 298(1–4), 242–266.

Di Luzio, M., R. Srinivasan, and J. G. Arnold (2001), *ArcView Interface for SWAT2000 - User's Guide*, Blackland Research Center, Texas Agricultural Experiment Station and Grassland, Soil and Water Research Laboratory, USDA Agricultural Research Service, Temple, Tex.

Döll, P., F. Kaspar, and B. Lehner (2003), A global hydrological model for deriving water availability indicators: Model tuning and validation, *J. Hydrol.*, 270(1–2), 105–134.

Esty, D. C., M. Levy, T. Srebotnjak, and A. de Sherbinin (2005), *2005 Environmental Sustainability Index: Benchmarking National Environmental Stewardship*, Yale Center for Environ. Law & Policy, New Haven, USA.

Falkenmark, M. (1989), The massive water scarcity now threatening Africe - Why isn't it being addressed?, *AMBIO*, 18(2), 112–118.

Falkenmark, M., and J. Rockström (2006), The new blue and green water paradigm: Breaking new ground for water resources planning and management, *J. Water Resour. Plann. Manage.*, 132(3), 129–132.

Falkenmark, M., and C. Widstrand (1992), Population and water resources: A delicate balance, *Popul. Bull.*, 47(3), 1–36.

Falkenmark, M., J. Lundquist, and C. Widstrand (1989), Macro-scale water scarcity requires micro-scale approaches: Aspects of vulnerability in semi-arid development, *Nat. Resour. Forum*, 13, 258–267.

FAO (Food and Agriculture Organization) (1995), *Digital soil map of the world and derived soil properties* [CD-ROM], Version 3.5, Land and Water Digital Media Series Number 1, Rome, Italy.

FAO (Food and Agriculture Organization) (2003), Review of the world water resources by country, *Water Report 23*, Rome, Italy. (Available at ftp://ftp.fao.org/agl/aglw/docs/wr23e.pdf)

Fekete, B. M., C. J. Vörösmarty, and W. Grabs (1999), Global composite runoff fields of observed river discharge and simulated water balances, *Report No. 22*, Global Runoff Data Centre, Koblenz, Germany.

Gassman, P. W., M. R. Reyes, C. H. Green, and J. G. Arnold (2007), The soil and water assessment tool: Historical development, applications, and future research directions, *Trans. ASAE*, 50(4), 1211–1250.

Gerten, D., S. Schaphoff, U. Haberlandt, W. Lucht, and S. Sitch (2004), Terrestrial vegetation and water balance - Hydrological evaluation of a dynamic global vegetation model, *J. Hydrol.*, 286, 249–270.

Gerten, D., H. Hoff, A. Bondeau, W. Lucht, P. Smith, and S. Zaehle (2005), Contemporary "green" water flows: Simulations with a dynamic global vegetation and water balance model, *Phys. Chem. Earth*, 30, 334–338.

Güntner, A., J. Stuck, S. Werth, P. Döll, K. Verzano, and B. Merz (2007), A global analysis of temporal and spatial variations in continental water storage, *Water Resour. Res.*, 43(5), W05416, doi:10.1029/2006WR005247.

Islam, M. S., T. Oki, S. Kanae, N. Hanasaki, Y. Agata, and K. Yoshimura (2007), A grid-based assessment of global water scarcity including virtual water trading, *Water Resour. Manage.*, 21, 19–33.

Korzun, V. I., A. A. Sokolow, M. I. Budyko, K. P. Voskresensky, G. P. Kalinin, A. A. Konoplyanstev, E. S. Korotkevich, P. S. Kuzin, and M. I. L'vovich, (Eds.) (1978), *World Water Balance and Water Resources of the Earth*, UNESCO, Paris.

Krause, P., D. P. Boyle, and F. Bäse (2005), Comparison of different efficiency criteria for hydrological model assessment, *Adv. Geosci.*, 5, 89–97.

Lehner, B., and P. Döll (2004), Development and validation of a global database of lakes, reservoirs and wetlands, *J. Hydrol.*, 296(1–4), 1–22.

L'vovitch, M. I. (1974), *World water resources and their future (in Russian)*, Moscow, Mysl. English translation: R. L. Nace (1979), Washington, D. C., AGU, 415 pp.

Neitsch, S. L., J. G. Arnold, J. R. Kiniry, and J. R. Williams (2005), *Soil and Water Assessment Tool - Theoretical Documentation - Version 2005*, Grassland, Soil and Water Research Laboratory, Agricultural Research Service and Blackland Research Center, Texas Agricultural Experiment Station, Temple, Tex.

Nijssen, B., G. M. O'Donnell, D. P. Lettenmaier, D. Lohmann, and E. F. Wood (2001), Predicting the discharge of global rivers, *J. Clim.*, 14(15), 3307–3323.

Oki, T., and S. Kanae (2006), Global hydrological cycles and world water resources, *Science*, 313, 1068–1072.

Oki, T., Y. Agata, S. Kanae, T. Saruhashi, D. W. Yang, and K. Musiake (2001), Global assessment of current water resources using total runoff integrating pathways, *Hydrol. Sci. J.*, 46(6), 983–995.

Revenga, C., J. Brunner, N. Henninger, K. Kassem, and R. Payne (2000), *Pilot Analysis of Global Ecosystems: Freshwater Systems*, World Resour. Inst., Washington, D.C., USA.

Rijsberman, F. R. (2006), Water scarcity: Fact or fiction?, *Agric. Water Manage.*, 80, 5–22.

Rockström, J., and L. Gordon (2001), Assessment of green water flows to sustain major biomes of the world: Implications for future ecohydrological landscape management, *Phys. Chem. Earth Part B*, 26(11–12), 843–851.

Rockström, J., M. Lannerstad, and M. Falkenmark (2007), Assessing the water challenge of a new green revolution in developing countries, *PNAS*, 104(15), 6253–6260.

Savenije, H. H. G. (2004), The importance of interception and why we should delete the term evapotranspiration from our vocabulary, *Hydrol. Processes*, 18, 1507–1511.

Schuol, J., and K. C. Abbaspour (2007), Using monthly weather statistics to generate daily data in a SWAT model application to West Africa, *Ecol. Modell.*, 201, 301–311.

Schuol, J., K. C. Abbaspour, R. Srinivasan, and H. Yang (2008), Estimation of freshwater availability in the West African sub-continent using the SWAT hydrologic model, *J. Hydrol.*, 352, 30–49.

Shiklomanov, I. A. (2000), Appraisal and assessment of world water resources, *Water Int.*, 25(1), 11–32.

Shiklomanov, I. A., and J. Rodda (Eds.) (2003), *World Water Resources at the Beginning of the 21st Century*, Cambridge Univ. Press, New York.

Smakhtin, V., C. Revenga, and P. Döll (2004), Taking into account environmental water requirements in global-scale water resources assessments, *Comprehensive Assessment Research Report 2*, International Water Management Institute, Colombo, Sri Lanka.

Srinivasan, R., T. S. Ramanarayanan, J. G. Arnold, and S. T. Bednarz (1998), Large area hydrologic modeling and assessment. Part II: Model application, *J. Am. Water Resour. Assoc.*, 34(1), 91–101.

UNESCO (2006), Water a shared responsibility, *The United Nations World Water Development Report 2*, UNESCO-WWAP, Paris, France.

UN-Water/Africa (2006), African water development report 2006, Econ. Comm. for Afr., Addis Ababa.

van Griensven, A., and T. Meixner (2006), Methods to quantify and identify the sources of uncertainty for river basin water quality models, *Water Sci. Technol.*, 53(1), 51–59.

Vörösmarty, C. J., C. A. Federer, and A. L. Schloss (1998), Evaporation functions compared on US watersheds: Possible implications for global-scale water balance and terrestrial ecosystem modeling, *J. Hydrol.*, 207(3–4), 147–169.

Vörösmarty, C. J., P. Green, J. Salisbury, and R. B. Lammers (2000), Global water resources: Vulnerability from climate change and population growth, *Science*, 289, 284–288.

Vörösmarty, C. J., E. M. Douglas, P. A. Green, and C. Revenga (2005), Geospatial indicators of emerging water stress: An application to Africa, *Ambio*, 34(3), 230–236.

Vrugt, J. A., H. V. Gupta, W. Bouten, and S. Sorooshian (2003), A Shuffled Complex Evolution Metropolis algorithm for optimization and uncertainty assessment of hydrologic model parameters, *Water Resour. Res.*, 39(8), 1201, doi:10.1029/2002WR001642.

Wagner, W., K. Scipal, C. Pathe, D. Gerten, W. Lucht, and B. Rudolf (2003), Evaluation of the agreement between the first global remotely sensed soil moisture data with model and precipitation data, *J. Geophys. Res.*, 108(D19), 4611, doi:10.1029/2003JD003663.

Wagner, W., G. Blöschl, P. Pampaloni, J.-C. Calvet, B. Bizzarri, J.-P. Wigneron, and Y. Kerr (2007), Operational readiness of microwave re-

mote sensing of soil moisture for hydrologic applications, *Nord. Hydrol.*, *38*(1), 1–20.

Wallace, J. S., and P. J. Gregory (2002), Water resources and their use in food production systems, *Aquat. Sci.*, *64*, 363–375.

Widén-Nilsson, E., S. Halldin, and C.-Y. Xu (2007), Global water-balance modelling with WASMOD-M: Parameter estimation and regionalisation, *J. Hydrol.*, *340*, 105–118.

Winchell, M., R. Srinivasan, M. Di Luzio, and J. G. Arnold (2007), *Arc-SWAT interface for SWAT2005 - User's guide*, Blackland Research Center, Texas Agricultural Experiment Station and Grassland, Soil and Water Research Laboratory, USDA Agricultural Research Service, Temple, Tex.

Yang, H., and A. J. B. Zehnder (2007), "Virtual water" - An unfolding concept in integrated water resources management, *Water Resour. Res.*, *43*(12), W12301, doi:10.1029/2007WR006048.

Yang, H., P. Reichert, K. C. Abbaspour, and A. J. B. Zehnder (2003), A water resources threshold and its implications for food security, *Environ. Sci. Technol.*, *37*(14), 3048–3054.

Yang, J., P. Reichert, K. C. Abbaspour, J. Xia, and H. Yang (2008), Comparing uncertainty analysis techniques for a SWAT application to the Chaohe basin in China, *J. Hydrol.*, doi:10.1016/j.jhydrol.2008.05.012, in press.

————————————

K. C. Abbaspour, J. Schuol, and H. Yang, Department System Analysis, Integrated Assessment and Modelling, Swiss Federal Institute of Aquatic Science and Technology (Eawag), P.O. Box 611, 8600 Dübendorf, Switzerland. (juergen.schuol@eawag.ch)

R. Srinivasan, Texas A&M University, Texas Agricultural Experimental Station, Spatial Sciences Laboratory, 1500 Research Plaza, College Station, TX 77845, USA.

A. J. B. Zehnder, Board of the Swiss Federal Institutes of Technology, ETH-Zentrum, Häldeliweg 15, 8092 Zürich, Switzerland.